Appl Microbiol Biotechnol
DOI 10.1007/s00253-016-7521-9

BIOENERGY AND BIOFUELS

Metabolic engineering of enhanced glycerol-3-phosphate synthesis to increase lipid production in *Synechocystis* sp. PCC 6803

Xi Wang[1] · Xiaochao Xiong[1] · Na Sa[2] · Sanja Roje[2] · Shulin Chen[1]

Received: 10 March 2016 / Accepted: 1 April 2016

Abstract With the growing attention to global warming and energy sustainability, biosynthesis of lipids by photosynthetic microorganisms has attracted more interest for the production of renewable transportation fuels. Recently, the cyanobacterium *Synechocystis* sp. PCC 6803 has been widely used for biofuel production through metabolic engineering because of its efficient photosynthesis and well-developed genetic tools. In lipid biosynthesis, glycerol-3-phosphate (G3P) is a key node for both CO_2 fixation and lipid metabolism in cyanobacteria. However, few studies have explored the use of G3P synthesis to improve photosynthetic lipid production. In this study, metabolic engineering combined with flux balance analysis (FBA) was conducted to reveal the effect of G3P synthesis on lipid production. Heterologous genes that encoded glycerol-3-phosphate dehydrogenase (GPD) and diacylglycerol acyltransferase (DGAT) were engineered into *Synechocystis* sp. PCC 6803 to enhance G3P supply and lipid production. The resultant recombinant *Synechocystis* produced higher levels of lipids without a significant reduction in cell growth. Compared with the wild-type strain, lipid content and productivity of the engineered cyanobacteria increased by up to 36 and 31 %, respectively, under autotrophic conditions. Lipid production under mixotrophic conditions of the engineered cyanobacteria was also investigated. This work demonstrated that enhanced G3P synthesis was an important factor in photosynthetic lipid production and that introducing heterologous GPD and DGAT genes was an effective strategy to increase lipid production in *Synechocystis* sp. PCC 6803.

Keywords Metabolic engineering · *Synechocystis* sp. PCC6803 · Glycerol-3-phosphate · Lipid synthesis · FBA

Introduction

The increasing effect of global warming and the unsustainable fossil fuel resources have raised attention to developing the eco-friendly renewable fuels. Integrating the processes for CO_2 capture with biosynthesis by photosynthetic microorganisms provides a promising strategy for producing carbon-neutral biofuels (Machado and Atsumi 2012; Parmar et al. 2011). Recently, the employment of photosynthetic cyanobacteria becomes an attractive option due to their efficient photosynthesis and flexibility of genetic modification for constructing a phototrophic cell factory (Atsumi et al. 2009; Ducat et al. 2011; Quintana et al. 2011). As a model cyanobacterium, *Synechocystis* sp. PCC 6803 is the first one with the complete genome sequenced and the well-illustrated genome-scale metabolic networks (Kaneko et al. 1996; Knoop et al. 2013). These advantages have made the *Synechocystis* become a new platform host strain to conduct sophisticated metabolic engineering for photosynthetic production (Yu et al. 2013). Consequently, *Synechocystis* has been engineered for the photosynthetic production of many biofuel molecules, such as lipids, fatty acids, fatty alcohols, alkanes, and isobutanol (Liu et al. 2011; Roberts et al. 2010; Tan et al. 2011; Varman et al. 2013a; Wang et al. 2013). Cyanobacteria can also be used to investigate the mechanisms of biosynthesis

Electronic supplementary material The online version of this article (doi:10.1007/s00253-016-7521-9) contains supplementary material, which is available to authorized users.

✉ Shulin Chen
chens@wsu.edu

[1] Department of Biological Systems Engineering, Washington State University, Pullman, WA 99164, USA

[2] Institute of Biological Chemistry, Washington State University, Pullman, WA 99164, USA

Published online: 07 May 2016

under phototrophic conditions because of its capability of photosynthetic functions (Ruffing 2011).

Chemically, lipids are favorable precursors for subsequent processes in fuel and oleochemical industry (Chisti 2007). This is because lipids can be converted to hydrocarbons such as alternative transportation fuels, and provides carbon skeletons for a range of oleochemicals (Hu et al. 2008). Thus, improving lipid synthesis through genetic engineering is critical to increase feedstock supplies. In lipid biosynthesis pathways, acetyl-CoA and glycerol-3-phosphate (G3P) are fundamental precursors for initializing fatty acid synthesis and triacylglycerol (TAG) formation, respectively (Courchesne et al. 2009). To increase lipid production, manipulating acetyl-CoA has been widely used as strategies in metabolic engineering, such as the enhancement of carbon flux from acetyl-CoA to fatty acid synthesis and the maintenance of the acetyl-CoA pool (Blazeck et al. 2014; Tai and Stephanopoulos 2013; Tang et al. 2013). However, few studies have explored the use of G3P synthesis to improve lipid production. In the yeast *Yarrowia lipolytica*, it was demonstrated that G3P played an important role in heterotrophic lipid synthesis because the acylation of G3P initializes TAG synthesis (Dulermo and Nicaud 2011). In the cyanobacterium *Synechocystis* sp. PCC 6803, G3P is mainly synthesized from dihydroxyacetone phosphate (DHAP) in the absence of glycerol (Nogales et al. 2012). The reaction between DHAP and G3P catalyzed by glycerol-3-phosphate dehydrogenase (GPD) could serve as a key node for both the Calvin-Benson-Bassham cycle and lipid synthesis (Fig. 1a). Therefore, G3P not only provides the glycerol backbone for TAG molecules in photosynthetic microorganisms but it may also play an important role in carbon partitioning by directly linking CO_2 fixation pathway to lipid synthesis.

Lipid synthesis is a complex process due to the repeated elongations of the carbon chain and the multi-step assembly for TAG; thus, additional tools are required to assist the metabolic engineering of the related process. The rapid development of metabolic flux modeling tools and metabolic network reconstructions has provided possibilities for the simulation of complex metabolic pathways. Applying constraint-based modeling methods such as flux balance analysis (FBA), the reconstructed metabolic networks can be used for the prediction of cellular metabolism (Orth et al. 2010). A growing number of studies have applied genome-scale modeling for conducting rational metabolic engineering (Ranganathan et al. 2012; Xu et al. 2011; Yim et al. 2011). For *Synechocystis* sp. PCC 6803, the reconstructed metabolic networks have been well developed with continuous efforts on updating current knowledge (Fu 2009; Knoop et al. 2010; Saha et al. 2012). One recent reconstruction (iJN678) for *Synechocystis* sp. PCC 6803 integrated completed fatty acid synthesis (Nogales et al. 2012), which enables the quantitative understanding of flux distribution and further investigation of the effects of G3P synthesis on lipid production.

In this study, the well-characterized GPD gene (*GPD1*) from *Saccharomyces cerevisiae* along with the gene *atf1* encoding diacylglycerol acyltransferase (DGAT) from oleaginous bacteria *Rhodococcus opacus* PD630 was introduced

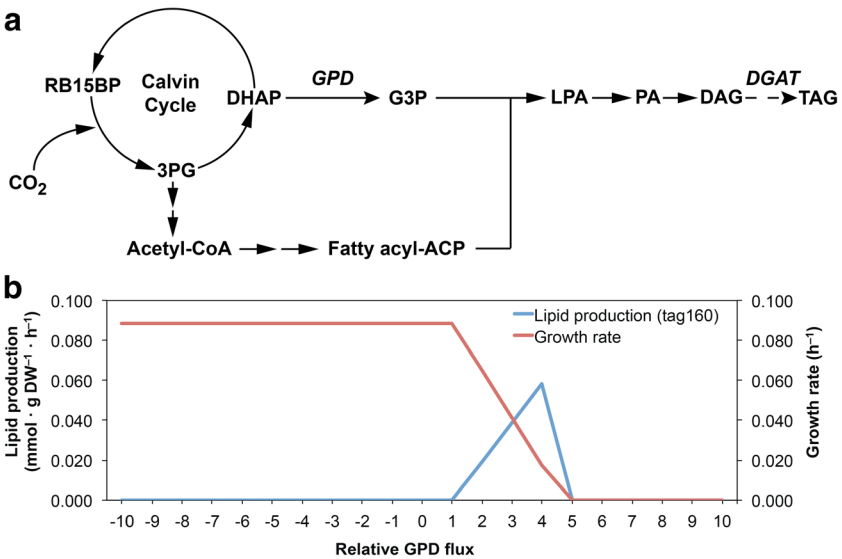

Fig. 1 Metabolic analysis of phototrophic lipid synthesis in *Synechocystis* sp. PCC 6803. **a** Metabolic pathway of lipid synthesis in *Synechocystis* sp. PCC 6803. *RB15BP* ribulose 1,5-bisphosphate, *3PG* 3-phosphoglycerate, *DHAP* dihydroxyacetone phosphate, *G3P* glycerol-3-phosphate, *LPA* lysophosphatidic acid, *PA* phosphatidic acid, *DAG* diacylglycerol, *TAG* triacylglycerol, *GPD* glycerol-3-phosphate dehydrogenase, *DGAT*diacylglycerol acyltransferase. **b** Simulation of the effect of G3P synthesis on lipid production under autotrophic conditions. *X*-axis represents the relative GPD flux, which is the ratio of test GPD flux to native GPD flux. Relative GPD flux = 1 served as the control (or native GPD flux), and relative GPD flux = 0 represented the blocked GPD reaction

into the cyanobacterium *Synechocystis* sp. PCC 6803 to enhance G3P supply and lipid production (Alvarez et al. 2008; Remize et al. 2001). The content of lipids produced by the engineered cyanobacteria was determined under both autotrophic and mixotrophic conditions. In addition, FBA was used to reveal the effect of enhanced G3P synthesis on lipid and cellular metabolism. Our intent was to demonstrate a possible strategy for increasing photosynthetic lipid production through metabolic engineering. Ideally, this strategy for improving lipid contents would not compromise cell growth in the engineered *Synechocystis*.

Materials and methods

Strains, medium, and culture conditions

All *Synechocystis* sp. PCC 6803 strains were grown in the BG-11 medium at 25 °C under a light intensity of 30 μmol photons s^{-1} m^{-2}. BG-11 plates also contained 15 g L^{-1} agar, 10 mM TES-NaOH (pH 8.2), and 3 g L^{-1} sodium thiosulphate (Eaton-Rye 2004). Twenty-five to 50 μg mL^{-1} of kanamycin was added to the BG-11 medium for recombinant selection when required. *Escherichia coli* NEB 5α was used for all plasmid construction. *E. coli* cells were grown on the Luria-Bertani (LB) medium at 37 °C. One hundred micrograms per milliliter of ampicillin or 50 μg mL^{-1} of kanamycin was added to the LB medium as needed. Information on strains used in this study is shown in Table 1.

For lipid production under autotrophic conditions, 150 mL liquid culture was grown in 250-mL flasks bubbled with a consistent 1 % CO_2-enriched air. For the mixotrophic culture, 50 mL of liquid BG-11 culture containing 30 mM D-glucose was grown in 250-mL flasks on a shaker in ambient air under light (Varman et al. 2013a). Cell growth was monitored by measuring optical density at 730 nm (OD 730 nm).

Plasmid construction and transformation of *Synechocystis* sp. PCC 6803

The plasmid pUC57 (GENEWIZ, South Plainfield, NJ, USA) was used for all DNA-fragment cloning (Table 2). Genes encoding GPD (*GPD1*, YDL022W) and DGAT (*atf1*, GQ923886) were cloned from the genomic DNA of *S. cerevisiae* FGSC 9721 and *R. opacus* PD630, respectively. *GPD1* and *atf1* genes were expressed constitutively under a *tac* promoter (P_{tac}). Primers (tac-GPD-F, tac-GPD-R) and primers (tac-atf-F, tac-atf-R) were used to clone the P_{tac} for *GPD1* and *atf1* genes, respectively. The reported consensus ribosome binding site (RBS) of *Synechocystis* sp. PCC 6803 (sequence, 5′-TTTAAAGGAGGTTAAAA-3′) was added just before the start codon (ATG), according to the information in Registry of Standard Biological Parts (BBa_K390002). The resultant plasmid pUC57-atf contains the expression cassette of *atf1*, including P_{tac}, consensus RBS sequence, and the coding sequence of *atf1*. Similarly, the constructed plasmid pUC57-GA contains both the expression cassettes of *atf1* and *GPD1* driven by P_{tac} individually. The plasmid pMIC003, which was used for the genetic transformation of *Synechocystis* sp. PCC 6803, contains the homologous recombination arms (5′-NS1, 3′-NS1). The expression cassette(s) from pUC57-atf and pUC57-GA were subcloned into the site of *SpeI* of plasmid pMIC003 to generate pNX1-atf and pNX1-GA plasmids, respectively. All oligonucleotides were ordered from Life Technologies (Grand Island, NY, USA).

Transformation of *Synechocystis* sp. PCC 6803 was performed by following the procedure, as described (Eaton-Rye 2004). Briefly, *Synechocystis* cells of exponential growth phase (OD 730 nm < 0.5) were harvested by centrifugation at 2760×*g* for 5 min at room temperature. The cell pellets were re-suspended at a final density of 1×10^9 cell mL^{-1} using fresh BG-11 medium. Two to 10 μg of plasmid DNA was added in 0.5 mL of cells suspension, and the mixture was placed at 30 °C under the light for 6 h. The *Synechocystis* cell mixture was then spread onto antibiotic-free BG-11 plates with Nuclepore membranes (Whatman, Florham Park, NJ, USA) for 12 h growth. The membranes were then transferred onto BG-11 plates containing 10–20 μg mL^{-1} of kanamycin. After 1–2 weeks incubation, the appeared single colonies were restreaked on plates for full segregation of the transformants. To verify the integration of engineered DNA fragment into the chromosome, diagnostic PCR was performed using specific primers (NS1-F, NS1-R)

Table 1 Strains used in this study

Strain name	Relevant genotype	Reference
Escherichia coli NEB 5α	*fhuA2 Δ(argF-lacZ)U169 phoA glnV44 Φ80 Δ(lacZ)M15 gyrA96 recA1 relA1 endA1 thi-1 hsdR17*	New England BioLabs, Inc.
Synechocystis sp. PCC 6803	Wild type	Targeted Growth, Inc.
Synechocystis sp. XW1	NS1:: P_{tac} *atf1* Km^R	This study
Synechocystis sp. XW2	NS1:: P_{tac} *GPD1* & *atf1* Km^R	This study

Km^R kanamycin resistance, *NS1* neutral site 1 of *Synechocystis* sp. PCC 6803

Table 2 Plasmids used in this study

Plasmid name	Relevant characteristics	Reference
pUC57	Km^R; *E.coli* cloning vector	Gene Wiz
pTAC-MAT-TAG-1	Amp^R; *E.coli* expression vector; source of *tac* promoter	Sigma-Aldrich
pMIC003	Amp^R; Km^R; Neutral site of *Synechocystis* sp. PCC 6803 (NS1) for homologous recombination	Targeted Growth, Inc.
pUC57-atf	Km^R; pUC57 derivative containing *atf1* gene; P_{tac} promoter;	This study
pUC57-GA	Km^R; pUC57 derivative containing *GPD1* and *atf1* genes; P_{tac} promoter	This study
pNX1-atf	Amp^R; Km^R; pMIC derivative containing *atf1* gene; P_{tac} promoter	This study
pNX1-GA	Amp^R; Km^R; pMIC derivative containing *GPD1* and *atf1* genes; P_{tac} promoter	This study

Amp^R ampicillin resistance, *Km^R* kanamycin resistance

with the extracted genomic DNA of recombinant *Synechocystis* as a template. Plasmids and primers used in this study are listed in Table 2 and Table S1.

Reverse transcription PCR

Synechocystis sp. PCC 6803 strains were grown in liquid BG-11 medium under autotrophic conditions (light and 1 % CO_2-enriched air supplied). The mid-log phase cells were used for total RNA extraction using a Purelink RNA Mini Kit, including the on-column Purelink DNase treatment (Life Technologies, Grand Island, NY, USA). Reverse transcription was performed using Omniscript RT Kit (Qiagen, Gaithersburg, MD, USA), with the addition of Recombinant RNasin Ribonuclease Inhibitor (Promega, Madison, WI, USA). Synthesized cDNA was then used as the template for a PCR test of the transcription of engineered genes. The housekeeping RNase P gene (*rnpB*) from *Synechocystis* sp. PCC 6803 was used as a control. Specific oligonucleotides used for reverse transcription PCR (RT-PCR) are listed in Table S2.

Enzymatic assay for glycerol-3-phosphate dehydrogenase

The procedure for the GPD assay was modified based on previously published methods (Gancedo et al. 1968). *Synechocystis* cells of mid-log growth phase were used to prepare crude cell extract. Cells were harvested by centrifugation at 4000×*g* and 4 °C for 10 min. The resulting cell pellets were re-suspended in a pre-chilled 10 mM EDTA (pH 7.0) buffer. Cells were disrupted with a bead beater (Mini Beadbeater, Biospec, Bartlesville, OK, USA), with the addition of 0.1-mm-diameter glass beads. After cell disruption, the isolated supernatant was used as crude cell extract by centrifugation at 12,000×*g*, 4 °C for 30 min (Angermayr et al. 2012). The enzymatic assay for GPD was prepared in a 200-μL reaction mixture containing 20 mM imidazol-HCl (pH 7.0), 0.1 mM NADH (Sigma-Aldrich, St. Louis, MO, USA), and 1.2 mM dihydroxyacetone phosphate (DHAP) (Sigma-Aldrich, St. Louis, MO, USA). Fresh crude cell extract was added to the reaction mixture to start the reaction, and oxidation of NADH was monitored at 340 nm and 30 °C in a 96-well microplate reader (SpectraMax Plus384, Molecular Devices, Sunnyvale, CA, USA). The quantification of protein content of crude cell extract was based on a comparison to a standard curve prepared with bovine serum albumin by using Quick Start Bradford Assay (Bio-Rad, Hercules, CA, USA) at 595 nm. One unit of GPD activity was defined as the specific rate for the conversion of 1 nmol NADH per min, per mg protein (nmol min^{-1} mg^{-1} protein).

Lipid extraction and quantification

Total lipid extraction and transesterification were performed according to the procedure described previously (O'Fallon et al. 2007). Prepared fatty acid methyl esters (FAME) in hexane were transferred into glass vials for gas chromatography (GC) analysis. GC analysis of FAMEs was performed using an Agilent 7890A gas chromatography instrument, equipped with a flame-ionization detector (FID) and a FAMEWAX column (30 m × 320 μm × 0.25 μm) (Restek Corporation, PA, USA). The injector was kept at 260 °C with an injection volume of 1 μL. The split ratio was 30:1. Oven conditions were as follows: the initial temperature was 190 °C and was ramped to 240 °C at a rate of 5 °C min^{-1} then held at 240 °C for 20 min. The FID temperature was 250 °C. FAME standards (Sigma-Aldrich, St. Louis, MO, USA) were used to identify and quantify fatty acids, and the tridecanoic acid (C13:0) (Sigma-Aldrich, St. Louis, MO, USA) was used as the internal standard. The total lipids were presented by sum of seven FAMEs: methyl palmitate (C16:0), methyl palmitoleate (C16:1), methyl stearate (C18:0), methyl oleate (C18:1), methyl linoleate (C18:2), methyl γ-linolenate (C18:3 n6), and methyl linolenate (18:3 n9). Dry cell weight (DW) was measured after drying at 105 °C until a consistent weight was reached (Wang et al. 2011; Xiong et al. 2012). Lipid

content was presented by the percentage of total lipids over dry cell weight.

Flux balance analysis

A reconstructed metabolic network of *Synechocystis* sp. PCC 6803 iJN678 (Nogales et al. 2012) was used to perform all computations based on the COBRA toolbox v2.0.5 within MATLAB_R2012b (Schellenberger et al. 2011). All computations were performed on a Mac OS X 10.9. SBML Toolbox_4.1.0 and libSBML_5.7.0 were installed to access the Systems Biology Makeup Language. An LP solver was set to Gurobi_5.1.0.

For FBA analysis, simulation constraints followed the uptake rates of 3.7 mmol gDW^{-1} HCO_3^- and 100 mmol gDW^{-1} photons described from (Nogales et al. 2012) to represent the autotrophic conditions. Since palmitate (C16:0) is the major component of fatty acids in *Synechocystis* sp. PCC 6803 (Sheng et al. 2011), tripalmitin that is the triacylglycerol assembled by three molecules of palmitate (C16:0) (termed as tag160) was used to represent the cellular lipid in the simulation. To simulate the lipid synthesis, a reaction of tag160 synthesis from diacylglycerol (DAG) and a correlated demand reaction were added into iJN678. Autotrophic cell growth was used as the objective function for all optimization. To reveal the effect of enhanced G3P synthesis on lipid and cellular metabolism in cyanobacteria, relative GPD fluxes were used to perform the robustness analysis by FBA. Since ferredoxin-$NADP^+$ reductase (FNOR, see Table S3) is the main pathway for NADPH synthesis in *Synechocystis* (Ducat et al. 2011), it was used to estimate the production level of NADPH through FBA analysis.

Results

Simulation of the effect of G3P synthesis on lipid synthesis

The simulation results show that in autotrophic conditions, increased GPD flux (or G3P synthesis) can improve lipid production yield along with a decrease in growth rate (Fig. 1b). Since overaccumulation of lipids in vivo is usually triggered by environmental stresses at the expense of cell growth, a suboptimal cell growth rate from increased G3P synthesis is acceptable for improved lipid production yield (Feist et al. 2010). Although the results also show that excessive GPD flux can result in both the growth rate and lipid production yield going down to zero, it is not realistic in experiment because of the limited affinity of GPD for DHAP. In addition, it was observed that other possible GPD fluxes such as reversed GPD fluxes and blocked GPD pathway may not significantly affect either growth rate or lipid production. Consequently, the simulation results indicate that increased G3P synthesis is possible to improve cellular lipid production.

Genetic construction and characterization of the recombinant *Synechocystis* sp. PCC 6803

A schematic of the genetic construction is shown in Fig. 2a. Gel electrophoresis showed a successful integration of engineered DNA fragment into the chromosome of recombinant *Synechocystis* by diagnostic PCR (Fig. 2b). All strains are fully segregated, and the genetic stability study by PCR showed positive after five generations of autotrophic culture (~70 days) without adding antibiotics. The resulting recombinant *Synechocystis* bearing *GPD1* and *atf1* genes was named XW2, and the recombinant strain carrying only the *atf1* gene was named XW1. The RT-PCR results showed the successful transcription of both introduced genes in engineered cyanobacteria (Fig. 2c). The enzymatic assay for GPD activity was used to characterize the engineered *GPD1* gene in the recombinant strain. GPD activities for the wild-type (WT) and XW2 strains were 15.24 ± 0.45 and 26.20 ± 5.24 units, respectively (Table 3). An approximate 170 % of relative GPD activity was observed in the recombinant XW2 strain, with a resulting increase in GPD flux compared to the WT strain.

Lipid analysis showed that lipid content in the recombinant XW2 strain was up to 8.1 % of dry cell weight after a 75-h culture, which is about 36 and 20 % higher than that in the WT and XW1 strains, respectively (Fig. 3a). Compared to the recombinant XW1 bearing only the *atf1* gene, the higher increase in lipid content in the recombinant XW2 suggested that the enhanced G3P synthesis was important for lipid production in *Synechocystis*. On the other hand, cell growth study showed that the growth rate of WT strain (~0.033 h^{-1}) was higher than that of the XW2 strain (~0.028 h^{-1}) in the log phase (Fig. 3b). However, a 10-day culture showed no significant difference in cell growth profile between the recombinant XW2 and the WT strains, although a slight decrease of cell biomass was observed in the XW2 strain in the final few days (Fig. 3b). This finding supports the simulation results described above that enhanced G3P synthesis improves cellular lipid; however, the cell growth in the recombinants was not significantly affected as observed in the experiment.

Lipid production in the recombinant *Synechocystis* under autotrophic conditions

In the autotrophic lipid production, the productivity and yield of lipid in the XW2 strain are higher than that of the WT strain (Fig. 4a). After 8 days of culturing, the lipid titer of the XW2 strain culture was about 134.1 mg L^{-1}, which is ~31 % higher than that of the WT strain (102.6 mg L^{-1}). Table 4 compared lipid productivities

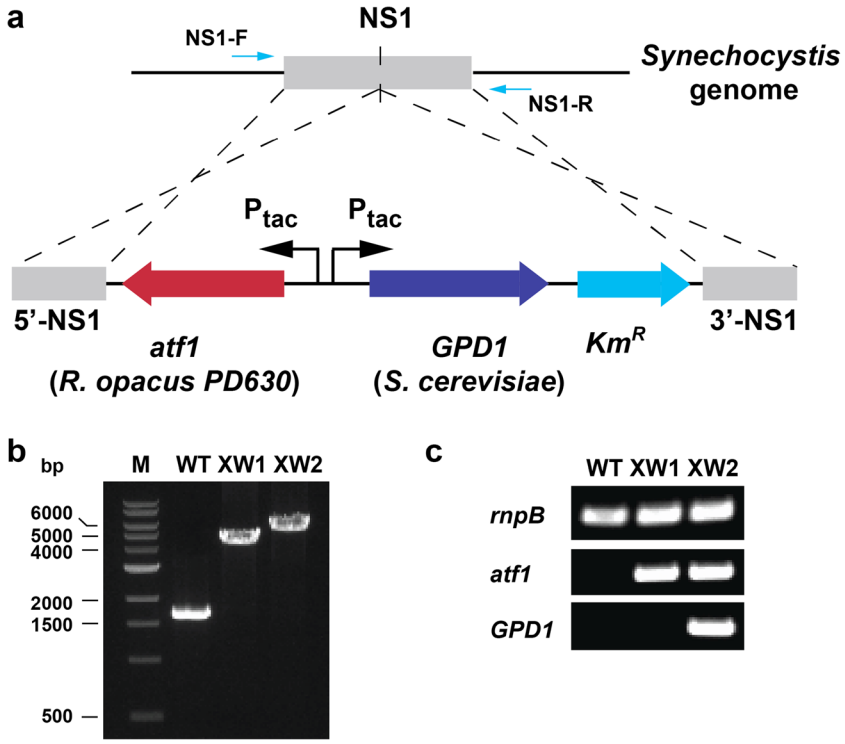

Fig. 2 Genetic construction of the recombinant *Synechocystis* strains. **a** Schematic of the engineered DNA fragment for homologous recombination in *Synechocystis*. 5′-NS1 and 3′-NS1 were homologous sequences at a neutral site (*NS1*) of *Synechocystis* sp. PCC 6803. NS1-F and NS1-R are primers used for diagnostic PCR. **b** Diagnostic PCR for verifying the integration of constructed DNA fragment into *Synechocystis* genome. **c** RT-PCR results. *WT* wild-type *Synechocystis* sp. PCC 6803. *XW1* recombinant strain bearing *atf1* gene, *XW2* recombinant strain bearing both *GPD1* and *atf1* genes

between XW2 and WT strains. The daily lipid production of XW2 and WT strains was about 16.8 and 12.8 mg L^{-1} day^{-1}, respectively. Profiling of fatty acid composition showed the source of the increased lipid titer. As shown in Fig. 4b, compared with the WT strain, the titers of palmitate (C16:0), linoleate (C18:2), and γ-linolenate (C18:3 n6) in the XW2 strain increased by 32, 33, and 14 %, respectively. An eightfold increase of oleate (C18:1) was also observed in the XW2 strain, which was surprising because oleate is not a dominant lipid component in *Synechocystis* sp. PCC 6803 (Sheng et al. 2011). The increased content of fatty acids can be attributed to the enhanced lipid synthesis, resulting from the improved availability of G3P and the introduced DGAT gene expression.

Lipid production in the recombinant *Synechocystis* under mixotrophic conditions

In the mixotrophic culture, cell growth of the recombinant strain XW2 was slightly slower than the WT strain (Fig. 5a). However, increased lipid production was also observed in the recombinant strain XW2 compared to the WT strain (Fig. 5b). The lipid titer of the XW2 strain was about 107.4 mg L^{-1}, which is ~20 % higher than that of the WT strain (89.6 mg L^{-1}). The results showed that the recombinant *Synechocystis* XW2 produced higher lipid than the WT strain under both autotrophic and mixotrophic conditions, which indicated that engineering of GPD and DGAT genes was an effective strategy for improving lipid production in *Synechocystis*.

Table 3 GPD activities in cell extracts of the WT and recombinant strains

Strain	GPD activity[a] (nmol min^{-1} mg^{-1} protein)	Relative activity (%)
Synechocystis sp. PCC 6803	15.24 ± 0.45	100
Synechocystis sp. XW2	26.20 ± 5.24	172

[a] Data are represented as average ± standard deviation ($n = 3$)

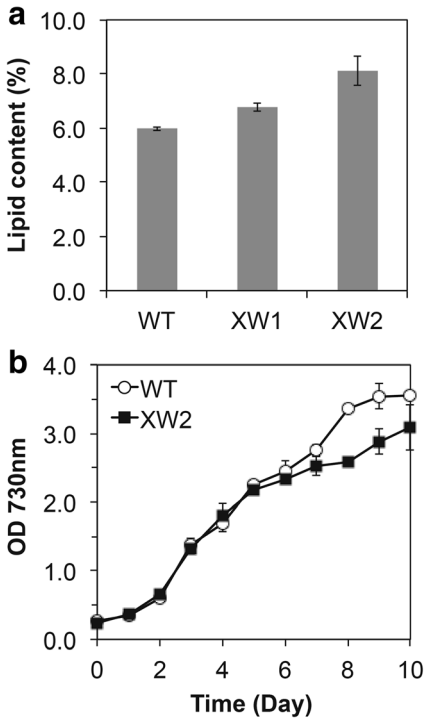

Fig. 3 Lipid content and cell growth of the recombinant *Synechocystis* under autotrophic conditions. **a** Lipid content (% of dry cell weight) represented by total lipids. **b** Cell growth curve (initial OD 730 nm = 0.2). *WT* wild-type *Synechocystis* sp. PCC 6803, *XW2* recombinant *Synechocystis* strain

Flux balance analysis for increased G3P synthesis

The effect of increased GPD flux on cellular metabolism was illustrated in Fig. 6. With the increase of relative GPD flux, improved fatty acid synthesis was observed in FBA analysis. In addition, slightly increased flux in carbon fixation (RuBisCO reaction) and decreased flux in photorespiration were observed through FBA, suggesting that CO_2 fixation may be improved with increased GPD flux. According to the in silico analysis, it was also found that NADPH production (FNOR reaction) was improved along with increased G3P synthesis. Although some results from this in silico flux analysis still need further experimental verification, such as the upregulated CO_2 fixation and downregulated flux distribution in the gluconeogenesis and part of the TCA cycle, it illustrates the possible mechanism for the contribution of carbon flux towards improved lipid production through enhancement of G3P synthesis.

Discussion

Metabolic engineering of enhanced G3P synthesis has been investigated in this study for improving photosynthetic lipid production in a model cyanobacterium *Synechocystis* sp. PCC 6803. Heterologous genes that encoded GPD and DGAT were engineered into *Synechocystis* sp. PCC 6803 to improve G3P synthesis and lipid production. The resulting recombinant *Synechocystis* XW2 strain showed an increase of 36 % in lipid content without a significant reduction in cell growth under autotrophic conditions. We also performed lipid production in the recombinant strain XW2 under mixotrophic conditions, observing a 20 % increase in lipid production compared to the wild-type strain.

The recombinant *Synechocystis* XW2 presented a modified fatty acid profile with a significant increase of oleate. This may be resulted from the substrate specificity of *atf1*-encoded DGAT, since an apparent reduced oleate was observed in an *atf1* disruption mutant of *R. opacus* PD630 (Alvarez et al. 2008). As TAG is the major storage molecule for lipids in vivo, DGAT, which catalyzes the synthesis of TAG from DAG, is considered as a key enzyme in lipid biosynthesis. Although cyanobacteria have a robust lipid synthesis metabolism for their photosynthetic membranes, their lack of lipid accumulation may be resulted from the lack of native DGAT gene(s) (Wada and Murata 1990). Introducing heterologous DGAT gene into *Synechocystis* sp. PCC 6803 has been proven

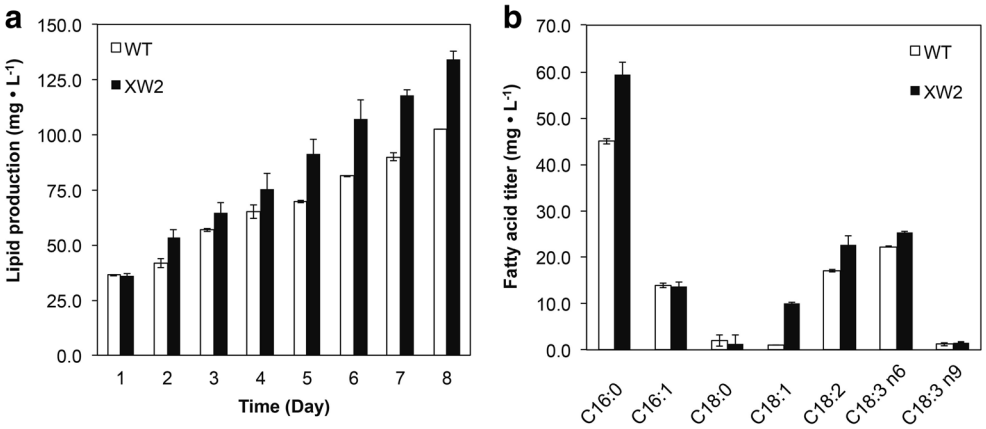

Fig. 4 Lipid production in the recombinant *Synechocystis* under autotrophic conditions. **a** Lipid production. Lipid production titer represented by total lipids. **b** Lipid profile after 8 days of culture. *WT* wild-type *Synechocystis* sp. PCC 6803, *XW2* recombinant *Synechocystis* strain

Table 4 Fatty acid productivity of the WT and recombinant strains

Fatty acids	Productivity (mg L^{-1} day^{-1})		Productivity/OD (mg L^{-1} day^{-1} OD^{-1})	
	WT	XW2	WT	XW2
C16:0	5.6	7.4	1.2	1.4
C16:1	1.7	1.7	0.4	0.3
C18:0	0.3	0.2	0.1	0.0
C18:1	0.1	1.2	0.0	0.2
C18:2	2.1	2.8	0.5	0.5
C18:3 n6	2.8	3.2	0.6	0.6
C18:3 n9	0.2	0.2	0.0	0.0
Total Lipid	12.8	16.8	2.8	3.2

WT wild-type *Synechocystis* sp. PCC 6803, *XW2* recombinant *Synechocystis* strain

for improving lipid accumulation (Roberts et al. 2010). Furthermore, our results demonstrate that increased G3P supply combined with DGAT gene expression is an effective strategy to enhance lipid production from CO_2 in *Synechocystis* sp. PCC 6803. The synergy between intensified GPD and DGAT expression in *Synechocystis* sp. PCC 6803 has a similar effect of the recently reported "push and pull" strategy to increase lipid accumulation, which was used for engineering improved lipid production in *Y. lipolytica* (Tai and Stephanopoulos 2013). Given codon optimization played an important role in the expression of heterologous genes in *Synechocystis* (Varman et al. 2013b), the optimal codon usage of heterologous genes could be critical to further improve the enzyme function and lipid yield.

Cell growth and biomass yield are important parameters in lipid production. In natural oleaginous microorganisms, lipid accumulation is usually triggered by limited nutrition (Papanikolaou and Aggelis 2011). Consequently, the increase in lipid content comes at the expense of cell growth or biomass yield, restricting further improvement of lipid production yield. In this study, we found that under the mixotrophic culture conditions, the recombinant XW2 strain showed a lower growth rate at the early culture phase, while the final cell biomass yield was similar compared to the WT strain. The improved biomass in the recombinant strain may be attributed to the enhanced lipid synthesis indirectly, through provision of more precursors such as phosphatidylglycerol (PG) for cell division (Domonkos et al. 2008). In addition, cell growth of the recombinants did not present a significant reduction under the autotrophic conditions. Thus, this study provides a possible strategy for metabolic engineering of increased cyanobacterial lipid production without compromising cell growth. Since there is no requirement for antibiotics, inducers, or limited nutrition to maintain increased lipid production, this strategy also shows promise for practical applications.

The glycerol backbone-derived three-carbon metabolites such as 3-phosphoglycerate (3PG), glyceraldehyde-3-phosphate (GAP), and G3P play a critical role in linking the metabolic pathways of carbon fixation, glycolysis, and lipid synthesis. In phototrophic lipid synthesis, GPD-

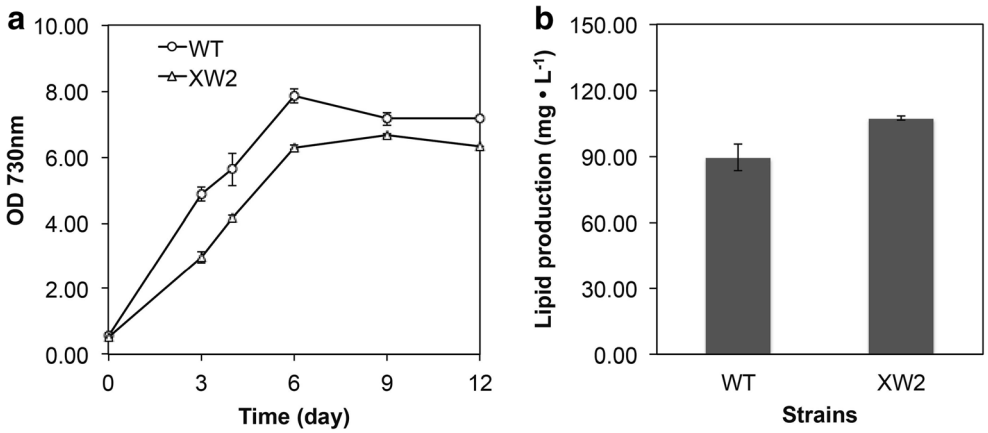

Fig. 5 Lipid production in the recombinant *Synechocystis* under mixotrophic conditions. **a** Cell growth curve. **b** Lipid production represented by total lipids. *WT* wild-type *Synechocystis* sp. PCC 6803, *XW2* recombinant *Synechocystis* strain

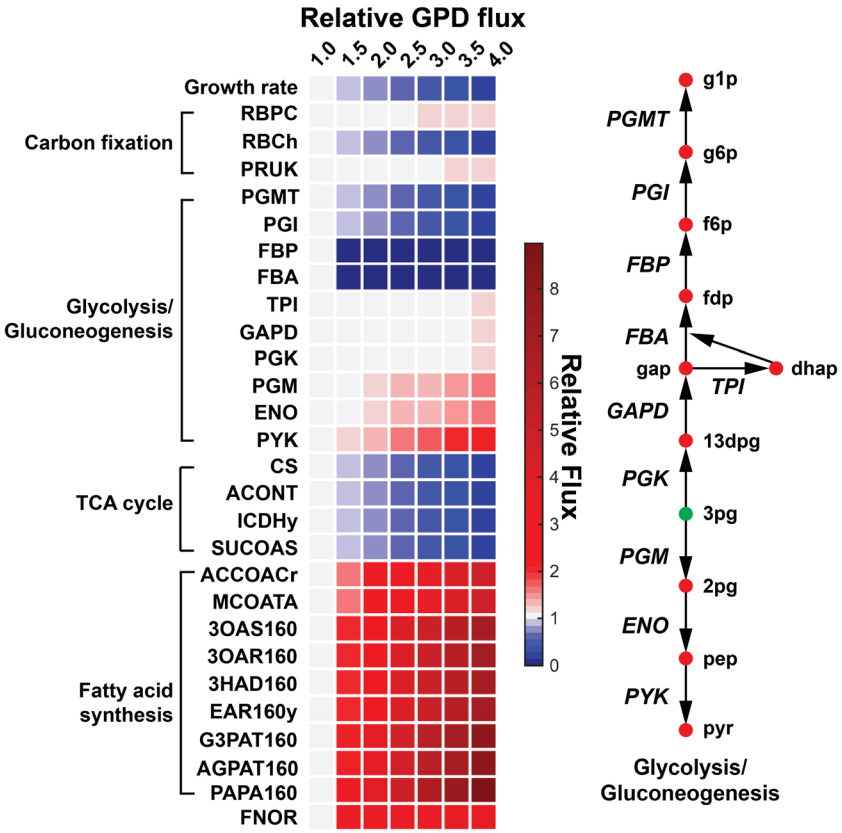

Fig. 6 Simulation of the impact of increased GPD flux on cellular metabolism for recombinant *Synechocystis* robustness analysis was investigated with increasing relative GPD fluxes (between 1 and 4). *X*-axis, relative GPD flux (the ratio of test GPD flux to native GPD flux). Relative GPD flux = 1.0 served as the control (or native GPD flux). *Y*-axis, relative flux of the pathways (the ratio of test flux to native flux). *Grey color* represents no change, *red color* represents upregulation, and *blue color* represents downregulation of the flux. The description of abbreviated reaction names was listed in Table S3. The schematic of the glycolysis/gluconeogenesis pathway shows the native reaction direction in *Synechocystis* sp. PCC 6803 under autotrophic conditions. *g1p* glucose 1-phosphate, *g6p* glucose 6-phosphate, *f6p* fructose 6-phosphate, *fdp* fructose 1,6-bisphosphate, *dhap* dihydroxyacetone phosphate, *gap* glyceraldehyde 3-phosphate, *13dpg* 1,3-bisphosphoglycerate, *3pg* 3-phosphoglycerate, *2pg* 2-phosphoglycerate, *pep* phosphoenolpyruvate, *pyr* pyruvate

catalyzed G3P synthesis links lipid synthesis to the carbon fixation pathway directly. Therefore, increased GPD flux may result in an improved conversion of CO_2 to lipid, since a higher RuBisCO flux (RBPC) was observed in the FBA simulation (Fig. 6). In addition, because glycerol is a major by-product in lipid-derived biodiesel production, the study of G3P synthesis provides an opportunity to recycle glycerol back into lipid production, in which G3P can be directly generated from glycerol by the catalytic activity of glycerol kinase.

In lipid biosynthesis, the elongations of carbon chain require a large amount of NADPH as reducing power, which is considered as a limiting factor. In heterotrophic prokaryotes such as *E. coli*, NADPH is mainly produced by glucose-6-phosphate/6-phosphogluconate dehydrogenase in pentose phosphate pathway, isocitrate-$NADP^+$ dehydrogenase in TCA cycle, and NAD(P) transhydrogenase (He et al. 2014). In oleaginous microorganisms such as *Y. lipolytica*, cytosolic malic enzyme also provides NADPH for lipid biosynthesis (Ratledge 2014). Interestingly, in phototrophic microorganisms such as *Synechocystis*, NADPH is predominantly produced by ferredoxin-$NADP^+$ reductase occurred in photosynthesis. Thus, the increased flux of ferredoxin-$NADP^+$ reductase observed in FBA analysis indicated more NADPH was produced, which could be supportive for the improved lipid synthesis (Fig. 6).

Applying genome-scale modeling to quantitatively analyze networked metabolites is one great advantage of FBA (Orth et al. 2010). Increasingly, the rapid advancement of reconstructed genome-scale models and the availability of metabolic flux modeling tools have attracted more attention from researchers. As a result, genome-scale modeling has been used in quantitative analysis and prediction related to metabolic engineering. By employing FBA to explore complex pathways, the effect of G3P synthesis on lipid and cellular metabolism was simulated. The identified mechanism of carbon flux towards the enhanced

lipid synthesis could be used to provide testable hypotheses for further optimization of robust cyanobacteria in photosynthetic lipid production. While FBA provides opportunities for in silico flux analysis, it only reflects the flux status at the steady state without kinetic parameters. The in silico flux distribution still has a significant difference from the results of ^{13}C metabolic flux analysis. Therefore, it is critical to further improve the quality of cyanobacterial constraint models for quantitative prediction of cellular metabolism.

Acknowledgments We would like to thank Targeted Growth, Inc. for the materials and technical support. We also want to thank the support from Gurobi Optimization, Inc., for academic users.

Compliance with ethical standards

Conflict of interest The authors declare that they have no conflict of interest.

Ethical approval This article does not contain any studies with human participants or animals performed by any of the authors.

References

Alvarez AF, Alvarez HM, Kalscheuer R, Waltermann M, Steinbuchel A (2008) Cloning and characterization of a gene involved in triacylglycerol biosynthesis and identification of additional homologous genes in the oleaginous bacterium *Rhodococcus opacus* PD630. Microbiology 154(8):2327–2335

Angermayr SA, Paszota M, Hellingwerf KJ (2012) Engineering a cyanobacterial cell factory for production of lactic acid. Appl Environ Microbiol 78(19):7098–7106

Atsumi S, Higashide W, Liao JC (2009) Direct photosynthetic recycling of carbon dioxide to isobutyraldehyde. Nat Biotechnol 27(12): 1177–1180

Blazeck J, Hill A, Liu L, Knight R, Miller J, Pan A, Otoupal P, Alper HS (2014) Harnessing *Yarrowia lipolytica* lipogenesis to create a platform for lipid and biofuel production. Nat Commun 5

Chisti Y (2007) Biodiesel from microalgae. Biotechnol Adv 25(3):294–306

Courchesne NMD, Parisien A, Wang B, Lan CQ (2009) Enhancement of lipid production using biochemical, genetic and transcription factor engineering approaches. J Biotechnol 141(1–2):31–41

Domonkos I, Laczkó-Dobos H, Gombos Z (2008) Lipid-assisted protein–protein interactions that support photosynthetic and other cellular activities. Prog Lipid Res 47(6):422–435

Ducat DC, Way JC, Silver PA (2011) Engineering cyanobacteria to generate high-value products. Trends Biotechnol 29(2):95–103

Dulermo T, Nicaud J-M (2011) Involvement of the G3P shuttle and beta-oxidation pathway in the control of TAG synthesis and lipid accumulation in *Yarrowia lipolytica*. Metab Eng 13(5):482–491

Eaton-Rye J (2004) The construction of gene knockouts in the cyanobacterium *Synechocystis* sp. PCC 6803. In: Carpentier R (ed) Photosynthesis research protocols, Methods In Molecular Biology™, vol 274. Humana Press, Totowa, NJ, pp. 309–324

Feist AM, Zielinski DC, Orth JD, Schellenberger J, Herrgard MJ, Palsson BØ (2010) Model-driven evaluation of the production potential for growth-coupled products of *Escherichia coli*. Metab Eng 12(3): 173–186

Fu P (2009) Genome-scale modeling of *Synechocystis* sp. PCC 6803 and prediction of pathway insertion. J Chem Technol Biotechnol 84(4): 473–483

Gancedo C, Gancedo JM, Sols A (1968) Glycerol metabolism in yeasts. Eur J Biochem 5(2):165–172

He L, Xiao Y, Gebreselassie N, Zhang F, Antoniewiez MR, Tang YJ, Peng L (2014) Central metabolic responses to the overproduction of fatty acids in *Escherichia coli* based on ^{13}C-metabolic flux analysis. Biotechnol Bioeng 111(3):575–585

Hu Q, Sommerfeld M, Jarvis E, Ghirardi M, Posewitz M, Seibert M, Darzins A (2008) Microalgal triacylglycerols as feedstocks for biofuel production: perspectives and advances. Plant J 54(4):621–639

Kaneko T, Sato S, Kotani H, Tanaka A, Asamizu E, Nakamura Y, Miyajima N, Hirosawa M, Sugiura M, Sasamoto S, Kimura T, Hosouchi T, Matsuno A, Muraki A, Nakazaki N, Naruo K, Okumura S, Shimpo S, Takeuchi C, Wada T, Watanabe A, Yamada M, Yasuda M, Tabata S (1996) Sequence analysis of the genome of the unicellular cyanobacterium *Synechocystis* sp. strain PCC6803. II Sequence determination of the entire genome and assignment of potential protein-coding regions. DNA Res 3(3):109–136

Knoop H, Gründel M, Zilliges Y, Lehmann R, Hoffmann S, Lockau W, Steuer R (2013) Flux balance analysis of cyanobacterial metabolism: the metabolic network of *Synechocystis* sp. PCC 6803. PLoS Comput Biol 9(6):e1003081

Knoop H, Zilliges Y, Lockau W, Steuer R (2010) The metabolic network of *Synechocystis* sp. PCC 6803: systemic properties of autotrophic growth. Plant Physiol 154(1):410–422

Liu X, Sheng J, Curtiss R III (2011) Fatty acid production in genetically modified cyanobacteria. Proc Natl Acad Sci U S A 109(7):2678–2683

Machado IMP, Atsumi S (2012) Cyanobacterial biofuel production. J Biotechnol 162(1):50–56

Nogales J, Gudmundsson S, Knight EM, Palsson BO, Thiele I (2012) Detailing the optimality of photosynthesis in cyanobacteria through systems biology analysis. Proc Natl Acad Sci U S A 108(17):6899–6904

O'Fallon JV, Busboom JR, Nelson ML, Gaskins CT (2007) A direct method for fatty acid methyl ester synthesis: application to wet meat tissues, oils, and feedstuffs. J Anim Sci 85(6):1511–1521

Orth JD, Thiele I, Palsson BO (2010) What is flux balance analysis? Nat Biotechnol 28(3):245–248

Papanikolaou S, Aggelis G (2011) Lipids of oleaginous yeasts. Part I: biochemistry of single cell oil production. Eur J Lipid Sci Technol 113(8):1031–1051

Parmar A, Singh NK, Pandey A, Gnansounou E, Madamwar D (2011) Cyanobacteria and microalgae: a positive prospect for biofuels. Bioresour Technol 102(22):10163–10172

Quintana N, Kooy F, Rhee M, Voshol G, Verpoorte R (2011) Renewable energy from cyanobacteria: energy production optimization by metabolic pathway engineering. Appl Microbiol Biotechnol 91(3):471–490

Ranganathan S, Tee TW, Chowdhury A, Zomorrodi AR, Yoon JM, Fu Y, Shanks JV, Maranas CD (2012) An integrated computational and experimental study for overproducing fatty acids in *Escherichia coli*. Metab Eng 14(6):687–704

Ratledge C (2014) The role of malic enzyme as the provider of NADPH in oleaginous microorganisms: a reappraisal and unsolved problems. Biotechnol Lett 36(8):1557–1568

Remize F, Barnavon L, Dequin S (2001) Glycerol export and glycerol-3-phosphate dehydrogenase, but not glycerol phosphatase, are rate limiting for glycerol production in *Saccharomyces cerevisiae*. Metab Eng 3(4):301–312

Roberts J, Cross F, Warrener P, Munoz EJ, Lee MH, Romari K (2010) Modified phototrophic microorganisms for producing triglycerides. US Patent US 2010/0081178A1

Ruffing AM (2011) Engineered cyanobacteria: teaching an old bug new tricks. Bioengineering 2(3):136–149

Saha R, Verseput AT, Berla BM, Mueller TJ, Pakrasi HB, Maranas CD (2012) Reconstruction and comparison of the metabolic potential of cyanobacteria *Cyanothece* sp. ATCC 51142 and *Synechocystis* sp. PCC 6803. PLoS One 7(10):e48285

Schellenberger J, Que R, Fleming RMT, Thiele I, Orth JD, Feist AM, Zielinski DC, Bordbar A, Lewis NE, Rahmanian S, Kang J, Hyduke DR, Palsson BO (2011) Quantitative prediction of cellular metabolism with constraint-based models: the COBRA Toolbox v2.0. Nat Protoc 6(9):1290–1307

Sheng J, Vannela R, Rittmann BE (2011) Evaluation of methods to extract and quantify lipids from *Synechocystis* PCC 6803. Bioresour Technol 102(2):1697–1703

Tai M, Stephanopoulos G (2013) Engineering the push and pull of lipid biosynthesis in oleaginous yeast *Yarrowia lipolytica* for biofuel production. Metab Eng 15(0):1–9

Tan X, Yao L, Gao Q, Wang W, Qi F, Lu X (2011) Photosynthesis driven conversion of carbon dioxide to fatty alcohols and hydrocarbons in cyanobacteria. Metab Eng 13(2):169–176

Tang X, Feng H, Chen WN (2013) Metabolic engineering for enhanced fatty acids synthesis in *Saccharomyces cerevisiae*. Metab Eng 16(0): 95–102

Varman AM, Xiao Y, Pakrasi HB, Tang YJ (2013a) Metabolic engineering of *Synechocystis* sp. strain PCC 6803 for isobutanol production. Appl Environ Microbiol 79(3):908–914

Varman AM, Yu Y, You L, Tang YJ (2013b) Photoautotrophic production of D-lactic acid in an engineered cyanobacterium. Microb Cell Factories 12(1):117

Wada H, Murata N (1990) Temperature-induced changes in the fatty acid composition of the cyanobacterium, *Synechocystis* PCC6803. Plant Physiol 92(4):1062–1069

Wang J, Zhang B, Chen S (2011) Oleaginous yeast *Yarrowia lipolytica* mutants with a disrupted fatty acyl-CoA synthetase gene accumulate saturated fatty acid. Process Biochem 46(7): 1436–1441

Wang W, Liu X, Lu X (2013) Engineering cyanobacteria to improve photosynthetic production of alka(e)nes. Biotechnol Biofuels 6(1):69

Xiong X, Wang X, Chen S (2012) Engineering of a xylose metabolic pathway in *Rhodococcus* strains. Appl Environ Microbiol 78(16): 5483–5491

Xu P, Ranganathan S, Fowler ZL, Maranas CD, Koffas MAG (2011) Genome-scale metabolic network modeling results in minimal interventions that cooperatively force carbon flux towards malonyl-CoA. Metab Eng 13(5):578–587

Yim H, Haselbeck R, Niu W, Pujol-Baxley C, Burgard A, Boldt J, Khandurina J, Trawick JD, Osterhout RE, Stephen R, Estadilla J, Teisan S, Schreyer HB, Andrae S, Yang TH, Lee SY, Burk MJ, Van Dien S (2011) Metabolic engineering of *Escherichia coli* for direct production of 1,4-butanediol. Nat Chem Biol 7(7):445–452

Yu Y, You L, Liu D, Hollinshead W, Tang Y, Zhang F (2013) Development of *Synechocystis* sp. PCC 6803 as a phototrophic cell factory. Mar Drugs 11(8):2894–2916